Emitter wrap-through solar cells – status and perspectives

Arne Fallisch[1], **James Gee**[2] & **Daniel Biro**[1]
[1]Fraunhofer Institute for Solar Energy Systems (ISE), Freiburg, Germany; [2]Applied Materials, Santa Clara, California, USA

ABSTRACT
Crystalline silicon wafer technology currently dominates industrial solar cell production. Common devices feature opposing electrodes situated at the front and the rear surface of the wafer, and subsequent front-to-rear interconnection is used for module assembly. This paper describes the status and perspectives of the emitter wrap-through (EWT) cell concept, which is a fully back-contacted solar cell. The functions which have to be fulfilled for this concept, as well as the corresponding challenges and advances, are discussed.

Introduction

Today crystalline silicon solar cells with classical front contacts form more than 80% of the market share of all PV technologies. The classical approach with a metallization grid on the front side, which in most cases consists of screen-printed silver, leads to shading losses. With the emitter wrap-through (EWT) solar cell concept, which was first published by Gee et al. [1] in 1993, these shading losses can be avoided and a larger amount of current can be extracted. Back-contact back-junction solar cells also avoid shading losses but feature more demanding requirements in terms of material quality, such as a high diffusion length of several times the cell thickness, which is necessary for achieving high efficiencies [2]. EWT cells already have an advantage over conventional cells when the diffusion length is about half the cell thickness [3]. This is due to the double-sided collection, made possible by front and rear emitters. An additional advantage offered by the full rear contacting is that an advanced module assembly can be used. This permits, for example, the use of wider tabs or foils for the cell interconnections, thus reducing the series resistance losses in the module [4,5].

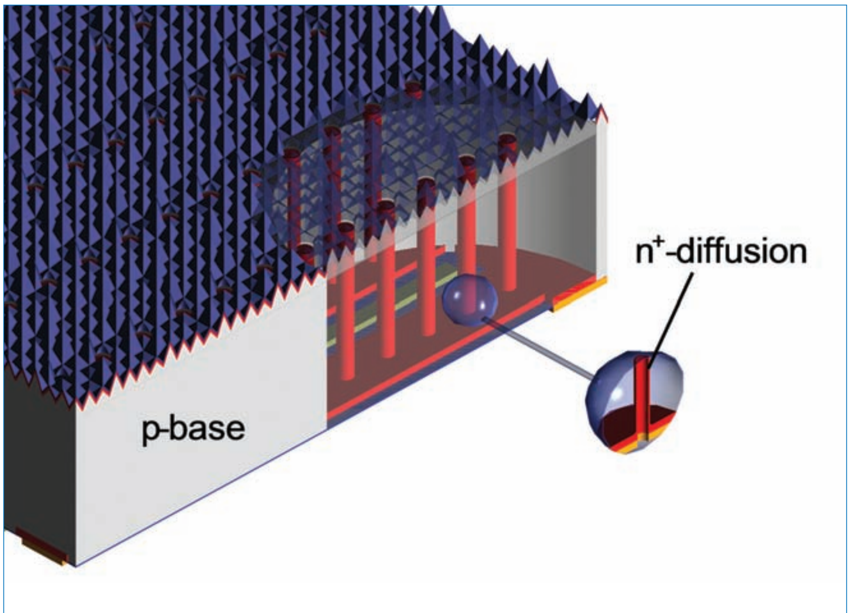

Figure 1. A 3-dimensional schematic view of an EWT solar cell [10].

> "With the emitter wrap-through (EWT) solar cell concept, shading losses can be avoided and a larger amount of current can be extracted."

Another way of increasing the conversion efficiency of conventional solar cells is to introduce passivation layers and local contacts as in the passivated and rear-emitter cell concept [6]. This can be combined with wrap-through concepts such as EWT. A combination of these improvements seems to be the most desirable for achieving high efficiencies beyond 20%. In the next section, the challenges and perspectives of manufacturing EWT solar cells will be addressed. Then, a review of recent cell results concerning the EWT concept will be presented, followed by a description of suitable cell design and module integration.

Challenges in manufacturing EWT solar cells

Manufacturing EWT solar cells is quite challenging, as their structure is more complex than that of conventional solar cells. A 3-dimensional schematic view of the EWT cell structure is shown in Fig. 1. To achieve the interconnection of the front emitter to the rear emitter, a set of densely placed via-holes (approximately 24300–48600 holes for a 243cm^2 wafer) has to be drilled. This is possible with today's advanced laser technology, as laser systems are already able to drill 5000 holes/s [7]. Considering the advances in laser technology, higher drilling rates than this will be likely in the future.

No laser-induced damage must remain inside the via-holes after the drilling step, since this leads to increased recombination [8,9]. The absence of damage can be ensured through a regular saw-damage removal step, which can also be used to achieve a flat rear surface.

Different approaches can be used to form the characteristic interdigitated pattern of the emitter on the rear side. Most publications report the formation of the grid using a patterned diffusion barrier of silicon dioxide or silicon nitride, for example. Of course, photolithography can be used to pattern this barrier; it makes the process rather expensive but the alignment accuracy is more precise. Other techniques – such as laser structuring [11], screen printing [12,13] or inkjet printing of an acid-resistant material – can be used to form the interdigitated pattern. To further reduce the number of process steps, direct printing of a diffusion barrier as shown by Spribille et al. [14] or Gee et al. [15] can be used.

The passivation of the pn-junction bordering the surface on the rear side is also an important issue. The length of the pn-junction can reach several metres on a wafer with an edge length of 125 or 156mm, depending on the distance between two fingers of the same polarity (often referred to as 'pitch'). As Kühn et al. [16,17] state, this leads to enhanced recombination depending on the quality of the surface passivation. It is therefore important to achieve a good passivation of the pn-junction on the rear side to achieve high efficiencies. Minigirulli [18] showed that an EWT cell with a passivated pn-junction has an increased conversion efficiency.

Another important issue is the metallization. Engelhart [11] showed a sophisticated self-aligned process using evaporated aluminium with a subsequent etching step. In this case the aluminium is used to contact both polarities. Account must therefore be taken of the fact that aluminium spiking effects on the emitter area might occur in subsequent low-temperature steps, leading to a decrease in cell efficiency [19,20]. Manole et al. [21] showed how the thermal stability of an evaporated aluminium contact can be increased using a thin tunnelling oxide layer or an aluminium-silicon alloy as a intermediate layer. Spiking effects can be circumvented by using screen-printed contacts. As already shown by several authors [15,18,22], screen printing with a subsequent co-firing step leads to functional EWT solar cells.

> "Precise alignment is a challenge that has to be met by the via-drilling and all patterning steps, to avoid possible shunting of the solar cells."

Precise alignment is a challenge that has to be met by the via-drilling and all patterning steps, to avoid possible shunting of the solar cells. In these terms a photolithographic patterning seems most desirable but on the other hand adds to the additional process complexity and costs. As Woehl et al. [23] state, with the screen-printing equipment and pastes used at Fraunhofer ISE, a pitch of 2mm for back-contact back-junction cells can be obtained with four alignment steps. For EWT cells, three alignment steps are possible but the alignment accuracy of the laser has to be taken into account as well. Fraunhofer ISE [23] have shown that pitches of 500µm width are possible using inkjet printing for back-contact back-junction cells.

With regard to all cell types reaching maximum cell efficiencies, the main optical and electrical loss mechanisms must be significantly reduced. While reducing the optical loss mechanisms is fairly simple, due to the absence of shading losses, the electrical loss mechanisms need to be looked at more closely. These losses can be split into electrical resistance and recombination losses and will be discussed next.

Electrical resistance

As in the case of all cell concepts, the electrical losses due to series resistance have to be kept as small as possible, which is rather challenging because lateral effects play an important role in the EWT cell. Lateral series resistance losses can be very high within the base, depending on the pitch of the interdigitated finger grid and the base resistivity: therefore the base resistivity and/or the pitch have to be quite low. If point contacts, for example laser-fired contacts [24], are used these losses will be even higher than for line contacts. Spreading resistance effects occur, leading to an enhanced series resistance of the cell [25]. On the other hand, a low base resistivity enhances the recombination in Cz silicon material due to the boron-oxygen complex [26]. The right choice of base material is therefore very important and depends on the pitch that can be realized with the patterning technology used.

Even more complex is the influence of the emitter sheet resistance in an EWT cell. Current crowding at the via-hole, which takes places at the front side [27], as well as series resistance losses due to the via-hole, increases the series resistance losses. According to Dicker [28] the series resistance losses due to the via-hole are one of the main loss mechanisms. But these losses can be reduced by increasing the number of via-holes. The arrangement of the via-hole pattern is also an important factor. Non-square via-hole patterns feature a larger amount of current transport in a single direction, which increases the contribution of the series resistance of the front side emitter to the total series resistance [29]. Therefore a square or hexagonal via-hole pattern with a high density of via-holes seems to be the most favourable. However, small pitches increase the length of the pn-junction on the rear surface and make the alignment more difficult.

The metallization on the rear side is another issue. For wafers with an edge length of 156cm, an interdigitated grid with one busbar on each side leads to high series resistance losses due to the large finger length. In this case the finger conductivity needs to be very high to reduce these losses to a minimum. A design with two busbar pairs as proposed by Kress et al. [22] can be used to reduce the finger length. Since the busbar is in most cases expanded, the current within the semiconductor has to travel a greater distance to reach the next contact, and consequently the region underneath the busbar contributes a larger portion to the total series resistance [30]. An alternative approach is therefore to use a busbar-less concept featuring conductive adhesives with a structured metal foil as proposed by Eickelbroom et al. [31]. This reduces the series resistance losses in a large-scale EWT solar cell and is one of the advantages over conventional cells.

Recombination

The emitter diffusion process is the key process, since it determines a great deal of the recombination losses.

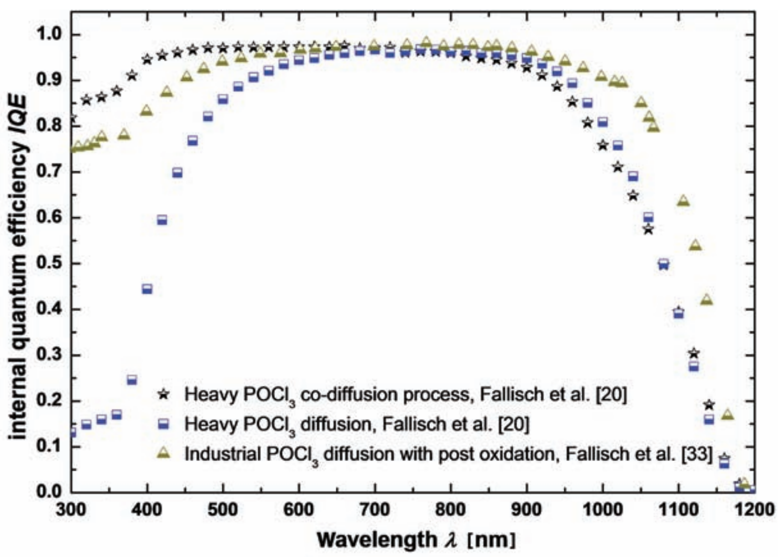

Figure 2. Measured IQE of an EWT cell for different diffused emitter profiles: a heavy diffusion process with and without a side selective emitter [20], and an industrial diffusion process with a subsequent oxidation [33].

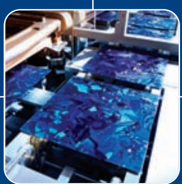
high speed

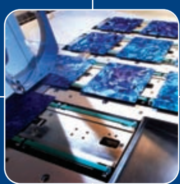
highest yields


print accuracy


compact footprint

Eclipse high throughput metallization solution

Combine six-sigma print accuracy with patented parallel print processing and an extremely COMPACT FOOTPRINT. What do you get? A high-speed solar metallization line that drives throughput beyond expected levels for the industry's best yields. Backed up by an unparalleled global infrastructure and award-winning service & support, DEK's Eclipse sets new productivity standards in solar cell manufacturing.

think beyond equipment.

For more information: www.deksolar.com

DEK® SOLAR

A DOVER COMPANY

Auger recombination is the main loss mechanism within the emitter because of the high density of charge carriers nearby. Therefore a low doping is preferable, which is in contradiction to a low series resistance. Furthermore, it has been shown by simulation that a high rear-emitter coverage is beneficial for the collection of minority charge carriers for low-quality material [32]. Hence it is even more important to have a very low emitter saturation current density. Engelhart [11] achieved emitter saturation current densities of approximately 130fA/cm^2 on a textured passivated front side and about 80fA/cm^2 on a planar oxide passivated rear side using a highly doped emitter. This leads to a peak open-circuit voltage of 668mV for the processed EWT cells.

> "The emitter diffusion process is the key process, since it determines a great deal of the recombination losses."

Moreover, a higher phosphorus doping and deep emitter on the front side not only enhances the Auger recombination, thereby reducing the open-circuit voltage, but also reduces the short-circuit current density due to reduced quantum efficiency in the short-wavelength range. This can be seen in Fig. 2, which shows three different internal quantum efficiency (IQE) measurements for different diffused emitter profiles.

Using a heavy diffusion process to obtain a high conductivity results in a low internal quantum efficiency in the short-wavelength range. If a co-diffusion process is used with a moderately doped front side emitter [20], the quantum efficiency can be significantly increased, leading to a higher short-circuit current density and in turn to a higher cell efficiency. Such a heavy diffusion process, however, is not necessary: an industrial diffusion process, which is used for conventional cells, can also be used for EWT cells. In this case a short oxidation step after the diffusion process and phosphosilicate glass (PSG) removal reduces the series resistance losses and the emitter recombination, and also passivates the pn-junction. Compared to cells featuring a heavy diffusion, an improved quantum efficiency is achieved, leading to short-circuit current densities of up to 39.5mA/cm^2. Of course, this industrial diffusion process can also be used as a co-diffusion process to further increase the quantum efficiency in the short-wavelength range.

Additional fill factor losses occur if the potential difference between the front and the rear of the pn-junction increases. This is an effect not only of an increased series resistance but also of an enhanced recombination. Due to the potential difference across the front and rear of the pn-junction, charge carriers in the front emitter are reinjected into the base material, where they diffuse to the rear side and are collected by the rear junction. This enhances the possibility of recombination, which leads to an additional decrease in fill factor. This effect appears particularly in the p-busbar regions, as the distance to the first row of via-holes is greater, which results in a larger difference in the voltage potential [30]. The same effect can appear if the base resistivity is too high and the potential difference in the lateral direction within the base increases. These via-resistance-induced recombination enhancements [34,35] or non-generation losses [36] depend on the geometrical parameters – such as pitch, number of holes and so on – as well as on the emitter resistivity and the base resistivity of the manufactured EWT cell. These effects can be avoided by choosing the right materials and geometries.

Review of EWT research

Since 1993 a lot of research has been done concerning the potential of EWT silicon solar cells. Gee et al. simulated a maximum efficiency of 21.6%, assuming Cz p-type material with a rather low value of 0.25Ωcm^2 for the lumped series resistance [1]. Several groups have since issued reports about the processing of EWT cells: a selection of these publications will now be reviewed.

In 1998 Smith et al. demonstrated an efficiency of 18.2% on an area of 41cm^2 – a record result at the time. The cells were made of float zone (FZ) silicon material. Photolithographic patterning of silicon dioxide was used to create the interdigitated grid on the rear side, and a heavy diffusion process was used to obtain a high conductivity. For metallization, an evaporated metal stack was used. In 2000 Kress et al. [37] reported an EWT solar cell efficiency of 16.1% on 10×10cm^2 Cz silicon material. This process sequence included two diffusion steps to achieve a moderately doped front emitter and a heavily doped emitter on the rear side and the via-holes. Screen printing was used for the metallization.

Just one year later, in 2001, Glunz et al. [38] presented the first EWT cell with a conversion efficiency exceeding 20%. On FZ silicon material, efficiencies of 21.4% have been achieved with an active cell area of 6cm^2. This cell featured a very high open-circuit voltage of 685mV and a short-circuit current density of 40.9mA/cm^2, but included a complex cell process with multiple diffusion and oxidation steps, and patterning using photolithography. Some years later, Kray et al. presented an EWT cell with an efficiency of 18.7% on Cz silicon with an active cell area of 6.23cm^2 after light-induced degradation [39]. However, these EWT cells also featured a cell process including photolithography patterning, several high-temperature steps and an evaporated metallization. These processes make the EWT cell rather expensive and not suitable for industrial production, but demonstrate the potential of the EWT structure in real devices.

In 2007 Engelhart [11] presented a calibrated measurement of 21.4% efficiency on an area of 92cm using FZ silicon. This cell had a very high short-circuit current density of 41.5mA/cm^2, which impressively showed the absence of shading losses and the advantages of the EWT cell concept. An open-circuit voltage of 668mV and a fill factor of 77.1% were also obtained. The patterning of the emitter and dielectric layers was performed using mask-free laser technology, and laser-fired contacts [24] were used on an evaporated aluminium metallization for the base contacts. As the process sequence also included four high-temperature steps (two diffusion and two oxidation steps) it was still very complex and therefore expensive. With a simpler process sequence that only included one oxidation and one diffusion step, a peak efficiency of 20.0% was achieved on the same area and material. On a large area of 125×125cm^2, the Institute for Solar Energy Research Hamelin (ISFH) reported a peak efficiency of 20.4% on FZ silicon material [40].

Mingirulli et al. presented a fully screen-printed EWT solar cell with 18.8% conversion efficiency on an area of 16.65cm^2 in 2009 [12,13]. Similar to the simpler fabrication process of Engelhart, the process sequence included only two high-temperature steps (one oxidation and one diffusion step). An industrial screen-printing process was used for the metallization. In the same year, Hacke et al. [5] reported results of a peak efficiency of 18.2% for an EWT cell on 156mm pseudo-square Cz silicon. On an area of 243cm^2, 17.2% has been achieved for multicrystalline material and 16.6% for upgraded metallurgical grade (umg) silicon (untextured).

Just recently, in 2011, Fallisch et al. [33] reported on an EWT cell on FZ silicon yielding a conversion efficiency of 18.7%, using a homogeneous industrial emitter diffusion process with a subsequent short oxidation after the PSG removal. The metallization consisted of a combination of screen printing and an evaporation process; this allowed a subsequent plating step for reducing series resistance losses. Both contacts were plated with silver, so soldering should be possible. On the other hand, an additional patterning step to isolate the evaporated contacts was necessary, which increased the process complexity.

Also in 2011, Gee et al. presented a peak conversion efficiency close to 19.8% before

light-induced degradation on a large area of 156×156cm^2 using Cz material [15]. The process sequence was rather short – it included an industrially-applicable back-to-back emitter diffusion step and screen-printed contacts. The process sequence included only a few extra process steps, such as laser drilling, protection of the rear side from an alkaline texturization process by a PECVD layer, printing of a diffusion barrier and a silicon nitride deposition on the rear side. These make the process sequence already usable for industrial application.

A little earlier in the year, the first n-type EWT cell with a peak conversion efficiency of 21.6% on a small area of 2×2cm^2 was presented by Kiefer et al. [41]. This cell featured a short-circuit current density of 40.4mA/cm^2, an open-circuit voltage of 661mV and a very high fill factor of 80.8%, which demonstrated that the EWT cell concept can also be successfully applied to n-type silicon material.

Cell design and module integration

Conventional silicon solar cells have their electrical contacts arranged in busbars on the front and rear surfaces that span the length of the cell. The cells are interconnected with flat Sn-coated Cu ribbon wire. To minimize optical losses, the ribbon must be made narrow; however, it cannot be made very thick, because the stiffness of thicker Cu ribbon will increase yield loss [42]. The compromise is to accept a rather high resistance loss of around 2% in conventional modules when using three busbars and 156mm cells. The optical loss is around 3% when using 1.6mm-wide Cu ribbon interconnects, three busbars and 156mm cells. The total loss associated with the interconnects is therefore approximately 5%.

One of the main advantages of back-contact cells is the minimization and/or elimination of the optical and resistive losses due to the interconnects when assembled into a module. Nevertheless, it is crucial to carry out the design of the cell and module together to maximize the cell and module performance. It should be remembered that most of this discussion is relevant to any back-contact solar cell technology – including back-contact back-junction cells and metallization-wrap-through (MWT) cells.

The first concepts of EWT cells used the same design paradigm as conventional cells. Busbars that ran the length of the cell were envisioned so that flat Cu ribbon interconnects could be used for module assembly [1]. The busbars could be placed at just the edges of the cell, or they could be included in the interior of the cell to reduce the average gridline length. A major problem was identified with

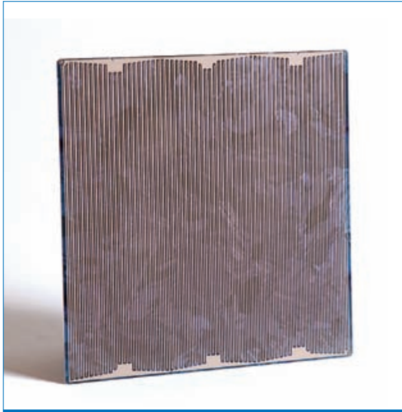

Figure 3. Rear surface of a 125mm EWT mc-Si cell.

busbars, specifically the regions of high resistance associated with the geometry [30]. The region over the busbars has a longer path length for current collection compared to the remaining active-area region. The equivalent circuit for a back-contact cell includes a solar cell with a high series resistance (representing the busbar regions) in parallel with a solar cell with low series resistance (representing the active-area regions). Some authors have since referred to this effect as 'electrical shading', although this term is also frequently used to refer to limitations in current collection due to finite diffusion lengths in back-contact back-junction solar cells [43]. It should be noted that some reported results for research devices use a 'designated area' measurement where the busbar regions are not illuminated during the measurement or included in the efficiency calculation to circumvent this loss mechanism. Such an approach, however, is obviously not applicable to commercial devices [44].

> "Good progress from both a cell and a module perspective has been made, bringing the EWT cell concept close to entering the market."

The series resistances losses can be minimized by reducing the area of the high-resistance regions, but this geometry change necessitates an alteration of the module assembly technology. The busbar dimensions can be minimized while still leaving pads for the electrical connections. An example of this geometry is shown in Fig. 3 for a 125mm EWT cell [45]. The tapering of the busbars allows current to be collected from the pads while minimizing the size of the busbars. This edge-connect geometry uses short, flat Cu interconnects between adjacent solar cells and for which modified stringer/tabber tools can be used. However, the series resistance of the solar cell is increased because of the very long grid lines.

Optimized for cost and performance, the design enables current to be collected and extracted from the solar cell in uniformly distributed locations throughout the interior of the cell [45]. Through refinement of this interior current-collection geometry and other improvements in the processing [15], efficiencies of up to 19.8% have been demonstrated for 156mm Cz EWT cells using only screen-printed metals and patterning. The cell layout was optimized for high efficiency, and the Ag metal usage minimized for cost reduction. The cell layout was also designed for use with a 'monolithic module assembly' that employs a large-area flexible circuit integrated with the module backsheet materials [46]. Many technical advantages of this approach have been previously described [47]. Rigorous (and in some cases new) testing procedures were implemented to ensure the reliability of such a new module assembly technology [45]. Modules built with a monolithic module assembly and EWT cells have passed and received IEC certification [46].

Conclusion

This article has shown which challenges have to be met for manufacturing EWT solar cells; the current status of EWT development has been reviewed. Most of the challenges, such as series resistance and recombination issues, are already known and, as pointed out, can be overcome by a suitable cell design and process sequence. One of the main advantages – the reduced shading losses – has been successfully demonstrated in several publications, with short-circuit current densities over 40mA/cm^2 being achieved. These current densities can be obtained using industrially diffused emitters.

Conversion efficiencies above 21% have already been realized on a small scale using mask-free patterning technology. On larger areas, the conversion efficiency achieved is close to 20% using a simple process sequence with only a few additional extra process steps. New approaches relating to the module assembly of back-contacted solar cells have produced suitable results, and monolithic module assemblies of EWT cells have received IEC certification. All these advances demonstrate that good progress from both a cell and a module perspective has been made, bringing the EWT cell concept close to entering the market.

References

[1] Gee, J.M., Schubert, W.K. and Basore, P.A. 1993, *Proc. 23rd IEEE PVSC*, Louisville, Kentucky, USA, p. 265.

[2] Granek, F. 2009, Ph.D. dissertation,


isishape®
Working with Sunshine™
The Efficient Alternative You Wanted!
Merck's printable etchants for advanced patterning for
• Selective Emitter
• MWT (Metal Wrap Through)
• LBSF (Local Back Surface Field)
• Edge Isolation
Easy, fast and environmentally friendly
www.isishape.com

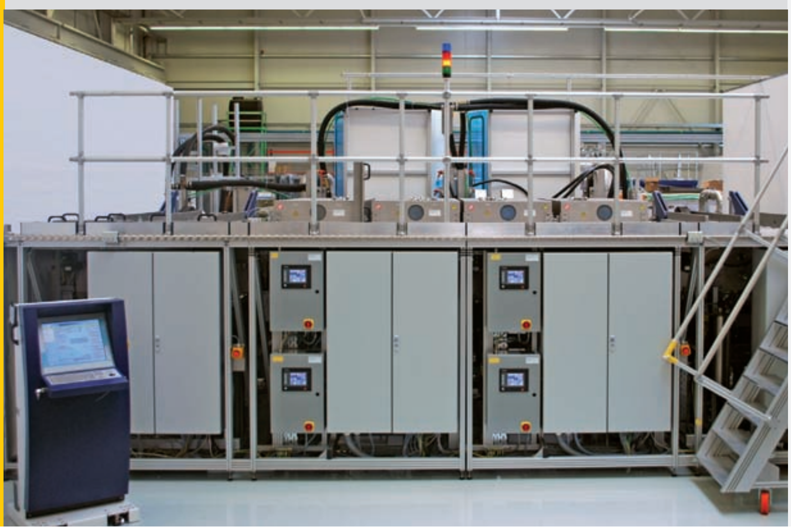

Institut für Mikrosystemtechnik, Albert-Ludwigs-Universität Freiburg, Freiburg, p. 209.
[3] Kerschaver, E., van Zechner, C. and Dicker, J. 2000, *IEEE Trans. Electron Dev.*, Vol. 47, p. 711.
[4] Clement, F. 2009, Ph.D. dissertation, Fakultät für Angewandte Wissenschaften, Universität Freiburg, Freiburg, p. 1.
[5] Hacke, P. et al. 2009, *Proc. 34th IEEE PVSEC*, Philadelphia, Pennsylvania, USA, p. 2102.
[6] Blakers, A.W. et al. 1989, *Appl. Phys. Lett.*, Vol. 55, p. 1363.
[7] Mayerhofer, R., Müllers, L. and Becker, A. 2006, *Proc. 4th WCPEC*, Waikoloa, Hawaii, USA, p. 1115.
[8] Mingirulli, N. et al. 2007, *Proc. 22nd EU PVSEC*, Milan, Italy, p. 1415.
[9] Mingirulli, N. et al. 2007, *Appl. Phys. Lett.*, Vol. 91, p. 183512/1.
[10] Glunz, S.W. 2007, *Adv. in OptoElectronics 2007*, p. 97370/1.
[11] Engelhart, P. 2007, Ph.D. dissertation, Fakultät für Elektrotechnik und Informatik, Universität Hannover, Germany, p. 162.
[12] Mingirulli, N. et al. 2011, *Prog. Photovolt. Res. Appl.*, Vol. 19, p. 366.
[13] Mingirulli, N. et al. 2009, *Proc. 24th EU PVSEC*, Hamburg, Germany, p. 1979.
[14] Spribille, A. et al. 2010, *Proc. 25th EU PVSEC*, Valencia, Spain, p. 2654.
[15] Gee, J.M. and Wang, M. 2011, *Proc. 26th EU PVSEC*, Hamburg, Germany.
[16] Kühn, R. et al. 1998, *Proc. 2nd World Conf. PV Energy Conver.*, Vienna, Austria, p. 1390.
[17] Kühn, R., Fath, P. and Bucher, E. 2000, *Proc. 28th IEEE PVSC*, Anchorage, Alaska, USA, p. 116.
[18] Mingirulli, N. 2009, Ph.D. dissertation, University of Konstanz, Konstanz, p. 54.
[19] Fallisch, A. et al. 2010, *Proc. 5th World Conf. PV Energy Conver.*, Valencia, Spain, p. 1991.
[20] Fallisch, A. et al. 2010, *Proc. 35th IEEE PVSC*, Honolulu, Hawaii, USA, p. 791.
[21] Manole, M. et al. 2005, *Proc. 20th EU PVSEC*, Barcelona, Spain, p. 1391.
[22] Kress, A. 2001, Ph.D. dissertation, Fachbereich Physik, Universität Konstanz, Konstanz, p. 131.
[23] Woehl, R. et al. 2010, *AIP Conf. Proc.*, Freiburg, Germany, Vol. 1277, p. 53.
[24] Schneiderlöchner, E. et al. 2001, *Proc. 17th EU PVSEC*, Munich, Germany, p. 1303.
[25] Fischer, B. 2003, Ph.D. dissertation, Fachbereich Physik, Universität Konstanz, Konstanz, p. 198.
[26] Schmidt, J., Aberle, A.G. and Hezel, R. 1997, *Proc. 26th IEEE PVSC*, Anaheim, California, USA, p. 13.
[27] Hall, R.N. and Soltys, T.J. 1980, *Proc. 14th IEEE PVSC*, San Diego, California, USA, p. 550.
[28] Dicker, J. 2003, Ph.D. dissertation, Fakultät für Physik, Universität Konstanz, Konstanz, p. 201.
[29] Fallisch, A. and Biro, D., *IEEE J. Photovoltaics* [forthcoming].
[30] Smith, D.D. et al. 1999, *IEEE Trans. Electron Dev.*, Vol. 46, p. 1993.
[31] Eikelboom, D.W.K. et al. 2001, *Proc. 17th EU PVSEC*, Munich, Germany, p. 1547.
[32] Hilali, M.M., Hacke, P. and Gee, J.M. 2006, *Proc. 4th World Conf. PV Energy Conver.*, Waikoloa, Hawaii, USA, p. 1299.
[33] Fallisch, A. et al. 2011, *Proc. 26th EU PVSEC*, Hamburg, Germany.
[34] Ulzhöfer, C. et al. 2010, *J. Appl. Phys.*, Vol. 107, p. 104509.
[35] Ulzhöfer, C. et al. 2008, *physica status solidi (RRL)*, Vol. 2, No. 6, pp. 251–253.
[36] Greulich, J. et al. 2011, *Proc. 1st Internat. Conf. Silicon PV*, Freiburg, Germany.
[37] Kress, A. al. 2000, *Proc. 28th IEEE PVSC*, Anchorage, Alaska, USA, p. 213.
[38] Glunz, S.W. et al. 2001, *Proc. 17th EU PVSEC*, Munich, Germany, p. 1287.
[39] Kray, D. et al. 2003, *Proc. 3rd World Conf. PV Energy Conver.*, Osaka, Japan, p. 1340.
[40] Institute for Solar Energy Research (ISFH) Hamelin 2007, Report, p. 92.
[41] Kiefer, F. et al. 2011, *Proc. 37th IEEE PVSC*, Seattle, Washington, USA.
[42] Zhao, J., Qi, W. and Ni, Z. 2011, *Photovoltaics International*, 12th Edn.
[43] Hermle, M. et al. 2008, *Proc. 33rd IEEE PVSC*, San Diego, California, USA, p. 1.
[44] Peters, C. et al. 2008, *Proc. 23rd EU PVSEC*, Valencia, Spain, p. 1010.
[45] Gee, J.M. et al. 2009, *Proc. 34th IEEE PVSC*, Philadelphia, Pennsylvania, USA, p. 002133.
[46] Meakin, D.H. et al. 2010, *Proc. 5th World Conf. PV Energy Conver.*, Valencia, Spain, p. 3858.
[47] De Jong, P. 2010, *Photovoltaics International*, 7th Edn.

About the Authors

Arne Fallisch studied information technology at the University of Wuppertal, Germany, and completed his master's degree in science at the Fraunhofer CalLab between November 2007 and May 2008. He continued with CalLab until November 2008, at which point he started working on his Ph.D. in engineering, with a focus on EWT silicon solar cells.

James Gee received a B.S. in electrical engineering from Rice University in Houston, Texas, and an M.S. in electrical engineering from Stanford University, California, USA. He has researched various areas of photovoltaic technology and managed a research team in crystalline silicon solar cell research while at Sandia National Laboratories. In 2003 James co-founded Advent Solar, the company responsible for introducing a back-contact multicrystalline-Si solar cell based on the EWT cell structure. He is currently chief scientist in crystalline-Si photovoltaics at Applied Materials in Santa Clara, California, USA.

Daniel Biro studied physics at the University of Karlsruhe, Germany, and at UMASS Amherst, USA. He completed his Ph.D. thesis on silicon solar cell diffusion technologies at the University of Freiburg, Germany, in 2003. In 2004/2005 Dr. Biro coordinated the design and ramp-up of the Fraunhofer production technology lab PV-TEC and is now head of the High Temperature and Printing Technologies/ Industrial Cell Structures department at Fraunhofer ISE.

Enquiries

PV Production Technology and Quality Assurance Department
Fraunhofer Institute for Solar Energy Systems
Heidenhofstrasse 2
79110 Freiburg
Germany
Tel: +49 (0) 761 4588 5272
Email: arne.fallisch@ise.fraunhofer.de
Website: www.ise.fraunhofer.de